



# HHS Public Access

Author manuscript

*Neurobiol Dis.* Author manuscript; available in PMC 2018 September 01.

Published in final edited form as:

*Neurobiol Dis.* 2017 September ; 105: 33–41. doi:10.1016/j.nbd.2017.05.007.

## Molecular Imaging of Serotonin Degeneration in Mild Cognitive Impairment

**Gwenn S. Smith, PhD,**

Department of Psychiatry and Behavioral Sciences, Johns Hopkins University School of Medicine, Baltimore, MD

Division of Nuclear Medicine, Russell H. Morgan Department of Radiology and Radiological Sciences, Johns Hopkins University School of Medicine, Baltimore, MD

**Frederick S. Barrett, PhD,**

Department of Psychiatry and Behavioral Sciences, Johns Hopkins University School of Medicine, Baltimore, MD

**Jin Hui Joo, MD,**

Department of Psychiatry and Behavioral Sciences, Johns Hopkins University School of Medicine, Baltimore, MD

**Najlla Nassery, M.D.,**

Department of Medicine, Division of General Internal Medicine, Johns Hopkins University School of Medicine, Baltimore, MD

**Alena Savonenko, MD, PhD,**

Department of Pathology (Neuropathology), Johns Hopkins University School of Medicine, Baltimore, MD

**Devin J. Sodums, MSc,**

---

Corresponding Author: Gwenn S. Smith, Ph.D., Department of Psychiatry and Behavioral Sciences, Division of Geriatric Psychiatry and Neuropsychiatry, Johns Hopkins University School of Medicine, Johns Hopkins Bayview Medical Center, 5300 Alpha Commons Drive, 4<sup>th</sup> floor, Baltimore, MD 21224, Phone: 410-550-6207, Fax: 410-550-1407, gsmith95@jhmi.edu.

**Publisher's Disclaimer:** This is a PDF file of an unedited manuscript that has been accepted for publication. As a service to our customers we are providing this early version of the manuscript. The manuscript will undergo copyediting, typesetting, and review of the resulting proof before it is published in its final citable form. Please note that during the production process errors may be discovered which could affect the content, and all legal disclaimers that apply to the journal pertain.

**Author Disclosures:**

Gwenn S. Smith, PhD has received research support from the National Institute of Health and Functional Neuromodulation, Inc.

Frederick S. Barrett, PhD reports no disclosures relevant to the manuscript

Christopher M. Marano, MD has received research support from the National Institute of Health

Jin Hui Joo, MD has received research support from the National Institute of Health

Cynthia A. Munro, PhD reports no disclosures relevant to the manuscript

Jason Brandt, PhD was a consultant to Neurotrope Bioscience, LLC and is a scientific consultant to MedAvante, Inc. He has received research support from the National Institutes of Health, Copper Ridge Institute, Douglas Hospital Research Center, and William and Ella Owens Medical Research Foundation. He has given expert testimony in the field of neuropsychology in a number of civil cases.

Alena Savonenko, MD, PhD has received research support from the National Institute of Health

Michael A. Kraut, MD, PhD reports no disclosures relevant to the manuscript

Yun Zhou, PhD reports no disclosures relevant to the manuscript

Dean F. Wong, MD, PhD has received research support from the National Institute of Health, Addex, Avid, Dart Neuroscience, Intracellular, Johnson and Johnson, Lilly, Lundbeck, Pfizer, Roche and Takeda

Clifford I. Workman, PhD reports no disclosures relevant to the manuscript

Najilla Nassery, MD reports no disclosures relevant to the manuscript

Department of Psychiatry and Behavioral Sciences, Johns Hopkins University School of Medicine, Baltimore, MD

**Christopher M. Marano, MD,**

Department of Psychiatry and Behavioral Sciences, Johns Hopkins University School of Medicine, Baltimore, MD

**Cynthia A. Munro, PhD,**

Department of Psychiatry and Behavioral Sciences, Johns Hopkins University School of Medicine, Baltimore, MD

**Jason Brandt, PhD,**

Department of Psychiatry and Behavioral Sciences, Johns Hopkins University School of Medicine, Baltimore, MD

**Michael A. Kraut, MD, PhD,**

Division of Neuroradiology, Russell H. Morgan Department of Radiology and Radiological Sciences Johns Hopkins University School of Medicine, Baltimore, MD

**Yun Zhou, PhD,**

Section of High Resolution Brain PET, Division of Nuclear Medicine, Russell H. Morgan Department of Radiology and Radiological Sciences, Johns Hopkins University School of Medicine, Baltimore, MD

**Dean F. Wong, MD, PhD, and**

Department of Psychiatry and Behavioral Sciences, Johns Hopkins University School of Medicine, Baltimore, MD

Section of High Resolution Brain PET, Division of Nuclear Medicine, Russell H. Morgan Department of Radiology and Radiological Sciences, Johns Hopkins University School of Medicine, Baltimore, MD

**Clifford I. Workman, PhD**

Department of Psychiatry and Behavioral Sciences, Johns Hopkins University School of Medicine, Baltimore, MD

## **Abstract**

Neuropathological and neuroimaging studies have consistently demonstrated degeneration of monoamine systems, especially the serotonin system, in normal aging and Alzheimer's disease. The evidence for degeneration of the serotonin system in mild cognitive impairment is limited. Thus, the goal of the present study was to measure the serotonin transporter *in vivo* in mild cognitive impairment and healthy controls. The serotonin transporter is a selective marker of serotonin terminals and of the integrity of serotonin projections to cortical, subcortical and limbic regions, as well as the cell bodies of origin (raphe nuclei).

Twenty-eight participants with mild cognitive impairment (age  $66.6 \pm 6.9$ , 16 males) and 28 healthy, cognitively normal, demographically matched controls (age  $66.2 \pm 7.1$ , 15 males) underwent magnetic resonance imaging for measurement of grey matter volumes and high-resolution positron emission tomography with well-established radiotracers for the serotonin transporter and regional cerebral blood flow. Beta-amyloid imaging was performed to describe, in

combination with the neuropsychological testing, the likelihood of subsequent cognitive decline in the participants with mild cognitive impairment. The following hypotheses were tested: 1) the serotonin transporter would be lower in mild cognitive impairment compared to controls in cortical and limbic regions, 2) in mild cognitive impairment relative to controls, serotonin transporter would be lower to a greater extent and more widespread than lower grey matter volumes or regional cerebral blood flow and 3) lower cortical and limbic serotonin transporters would be correlated with greater deficits in auditory-verbal and visual-spatial memory in mild cognitive impairment, not in controls.

Reduced serotonin transporter availability was observed in mild cognitive impairment compared to controls in cortical and limbic areas typically affected by Alzheimer's disease pathology, as well as in sensory and motor areas, striatum and thalamus that are relatively spared in Alzheimer's disease. The reduction of the serotonin transporter in mild cognitive impairment was greater than grey matter atrophy or reductions in regional cerebral blood flow compared to controls. Lower cortical serotonin transporters were associated with worse performance on tests of auditory-verbal and visual-spatial memory in mild cognitive impairment, not in controls.

The serotonin system may represent an important target for prevention and treatment of MCI, particularly the post-synaptic receptors (5-HT<sub>4</sub> and 5-HT<sub>6</sub>), which may not be as severely affected as presynaptic aspects of the serotonin system.

## Keywords

serotonin transporter; Positron Emission Tomography (PET); mild cognitive impairment; aging

## INTRODUCTION

Neuropathological and neuroimaging studies have consistently demonstrated degeneration of monoamine systems, in particular the serotonin system, in normal aging and in Alzheimer's disease (AD; as reviewed by Hirao et al., 2014). Neuropathological studies in AD demonstrate neurofibrillary tangles and loss of the cell bodies of origin of the cortical serotonin projections, the raphe nuclei (Curcio and Kemper, 1984, Mann and Yates, 1983). Lower cortical serotonin levels and metabolites (5-Hydroxyindoleacetic acid), serotonin transporters (SERT), 5-HT<sub>2A</sub> and 5-HT<sub>1A</sub> receptors are also observed in post-mortem studies in AD compared to controls (e.g. D'Amato et al., 1983, Thomas et al., 2006, Zweig et al., 1988, Marcusson et al., 1987, Tejani-Butt et al., 1995, Tsang et al., 2003, Palmer et al., 1988, Bowen et al., 1979, 1983). Serotonergic deficits are greater and more widespread than those of other neurotransmitters in AD, including other monoaminergic and cholinergic systems (Palmer et al., 1988, Cross et al., 1986, Baker and Reynolds, 1989, Nazarali and Reynolds, 1992). Neuroimaging studies have demonstrated lower global cortical 5-HT<sub>2A</sub> receptors (Blin et al., 1993) and lower 5-HT<sub>1A</sub> receptor in a more localized region of medial temporal cortex in AD compared to controls (Lanctot et al., 2007). Lower cortical and hippocampal 5-HT<sub>1A</sub> receptor availability is associated with greater cognitive impairment, lower hippocampal glucose metabolism and greater AD neuropathology (Kepe et al., 2006). Two studies of SERT have shown lower SERT in striatal and midbrain regions (to a greater extent in depressed than in non-depressed AD patients) and lower SERT in mesial temporal

cortex, respectively, in AD compared to controls (Ouchi et al., 2009, Marner et al., 2012). Thus, post-mortem and neuroimaging studies of the serotonin system in AD are concordant in the demonstrations of serotonin system degeneration in AD.

The evidence for degeneration of the serotonin system in mild cognitive impairment (MCI) is limited. As a result, it is not known whether serotonin degeneration occurs in the pre-clinical stages or later in the course of AD. Neuroimaging studies of the serotonin system in MCI have focused on the 5-HT<sub>1A</sub> and 5-HT<sub>2A</sub> receptors (Kepe et al., 2006, Truchot et al., 2008 and Hasselbalch et al., 2008). Lower 5-HT<sub>2A</sub> and 5-HT<sub>1A</sub> receptors in cortical and hippocampal regions, respectively, in MCI compared to controls have been observed in two studies (Hasselbalch et al., 2008, Kepe et al., 2006). In contrast, a third study reported higher cortical and hippocampal 5-HT<sub>1A</sub> receptors in MCI and lower higher cortical and hippocampal 5-HT<sub>1A</sub> receptors in AD (Truchot et al., 2008).

SERT has been a limited focus of study in AD and MCI. Neuroimaging of SERT may better elucidate degeneration of the serotonin system because SERT is a more specific marker of serotonin terminals and of the integrity of serotonin projections than are 5-HT<sub>1A</sub> or 5-HT<sub>2A</sub> receptors that are located on the terminals of non-serotonergic neurons (Azmitia and Nixon, 2008). Thus, measuring SERT would be more sensitive to changes intrinsic to the serotonin system than measuring 5-HT<sub>1A</sub>, 5-HT<sub>2A</sub> or other serotonin receptors that may be up- or down-regulated due to changes in other neurotransmitter systems (e.g. the cholinergic system; Quirion et al., 1985, 1987) or in response to a neuropathological process (e.g. cerebrovascular disease; Elliot et al., 2009). Further investigation of serotonin degeneration, particularly SERT in MCI, would have implications for whether serotonin degeneration may be a downstream effect of AD pathology or may have a causative role, especially regarding cognitive deficits and neuropsychiatric symptoms. Studies in amyloid transgenic mouse models have shown that cortical serotonin degeneration may precede substantial cortical deposition of beta-amyloid, as well as cortical and hippocampal cell loss, and may be observed early in the course of AD pathophysiology (Liu et al., 2008).

SERT is expressed on serotonin cell bodies and axons in the raphe nuclei and on pre-synaptic serotonin terminals (Blakely et al., 1998). Post-mortem autoradiography studies show high SERT concentrations in anterior cingulate, entorhinal and insular cortices and the temporal pole. Other regions of high SERT concentrations include the hippocampal formation (molecular layer and CA3 and external layers of the subiculum), medial caudate, putamen, ventral striatum, thalamus (anterior, medial-dorsal, midline and pulvinar nuclei), and raphe nuclei (Steinbusch, 1981, Varnäs et al., 2004). Thus, based on the neuroanatomy of the serotonin system, higher concentrations of SERT are observed in cortical and limbic regions and the midbrain serotonin cell bodies, that overlap with regions that show AD pathology (beta-amyloid and tau deposition and deficits in cerebral glucose metabolism in early disease (Arnold et al., 1991, Rub et al., 2000, Smith et al., 1992).

The present study measured SERT in participants with MCI and in demographically matched, healthy, cognitively normal comparison subjects using positron emission tomography (PET) and a well-established, selective radiotracer for SERT, [<sup>11</sup>C]-3-amino-4-(2-dimethylaminomethyl-phenylsulfanyl)-enzonitrile ([<sup>11</sup>C]-DASB; Wilson et al., 2002). To

determine whether the lower SERT in MCI compared to controls was observed in regions in which cerebral atrophy or lower regional cerebral blood flow (as an index of brain function) were seen, grey matter volumes were measured with magnetic resonance imaging (MRI) and regional cerebral blood flow (rCBF) was measured with PET using the radiotracer [ $^{15}\text{O}$ ]-water. Beta-amyloid imaging was performed in MCI using the radiotracer [ $^{11}\text{C}$ ]-PiB to describe, in combination with the neuropsychological testing, the likelihood of subsequent cognitive decline. To determine whether changes in SERT were associated with memory performance, SERT data were correlated with auditory-verbal and visual-spatial memory tests. To complement the voxel-wise analyses used in the study, exploratory factor analyses were performed with the region of interest data to determine whether the two analysis methods would provide converging results. The following hypotheses were tested: 1) that SERT will be lower in the cortical (frontal, temporal and parietal association cortices) and limbic (amygdala, hippocampus) brain regions in MCI compared to controls, 2) independent, exploratory factor analysis would show lower SERT in cortical regions in MCI compared to controls, consistent with the voxel-wise analysis; 3) reductions in SERT will be greater and more extensive than reductions in grey matter volumes or rCBF in MCI compared to controls, and 4) lower cortical and limbic SERT will be associated with greater memory impairment in MCI.

## MATERIALS AND METHODS

### Subject Screening and Selection

Participants were recruited from advertisements in the community or from the Johns Hopkins University Alzheimer's Disease Research Center (2P50AG005146). All subjects underwent psychiatric and cognitive evaluations, including a structured clinical interview by a clinical psychologist (SCID), clinical dementia rating scale (CDR), Mini Mental State Examination (MMSE) and Neuropsychiatric Inventory (NPI; First et al, 1995, Morris, 1993, Folstein et al., 1976, Cummings et al., 1994). All participants underwent a physical and neurological examination, laboratory testing (including complete blood count and blood chemistries), toxicology screening (psychotropic drugs and drugs of abuse) and MR imaging prior to the PET scans. Participants were excluded from the study who had a history of or active neurological or Axis I psychiatric disorders including substance abuse, who were not medically stable (i.e. if they had poorly controlled hypertension and/or insulin dependent diabetes), for a positive toxicology screening for psychotropic drugs or medications with central nervous system effects or if they used prescription or over-the-counter medications with potential central nervous system effects (e.g. antihistamines, cold medications) within the past two weeks prior to enrollment. The MCIs were required to have a CDR global score of 0.5, whereas the controls were required to have a CDR global score of 0 (normal). Twenty-eight participants with MCI and 28 healthy controls were enrolled. One of the controls and two of the MCIs were left handed. The study protocol and consent forms were approved by the Institutional Review Board and the Radiation Research Committee of the Johns Hopkins University School of Medicine. Participants received a transcribed and verbal description of the study and written informed consent was obtained.

## Neuropsychological Testing

All participants underwent neuropsychological testing within one week of the PET scans. The neuropsychological test battery included tests of executive function, attention, auditory-verbal and visual-spatial memory and decision making (data not shown). Two neuropsychological tests that assess memory and are sensitive to detecting memory impairment in MCI were used for correlation with the SERT data. The tests included the California Verbal Learning Test (CVLT, a test of auditory-verbal memory) and the Brief Visual memory Test-Revised (BVMT-R, a test of visual-spatial memory (Delis et al., 1988, Benedict, 1997)). The CVLT variable used for analysis was the total number of words recalled without perseverations and intrusions over the first five trials. Similarly, the BVMT-R variable that was analyzed was the number of shapes and their location recalled over three learning trials.

## MR Imaging Procedures

MR images of the brain were acquired using a Phillips 3.0T Achieva MRI instrument with an 8 channel head coil (Philips Medical Systems, Best, Netherlands) at the F. M. Kirby Research Center for Functional Brain Imaging of the Kennedy Krieger Institute. The magnetization-prepared rapid acquisition with gradient echo (MPRAGE) pulse sequence (TE = 4, TR = 8.9, flip angle = 8 degrees, NSA = 1, 0.7mm isotropic voxel size) was used for volumetric analyses and MR to PET co-registration.

## PET Imaging Procedures

PET scans were acquired at the PET Center, Russell H. Morgan Department of Radiology, Johns Hopkins University School of Medicine. The scanner used was a second-generation High Resolution Research Tomograph scanner (HRRT, Siemens Healthcare, Knoxville, TN), a cerium-doped lutetium oxyorthosilicate (Lu<sub>2</sub>SiO<sub>5</sub>[Ce] or LSO) based, dedicated brain PET scanner with two mm resolution. Each subject was fitted with a thermoplastic mask modeled to his or her face to reduce head motion during the PET study. The attenuation maps were generated from a six-minute transmission scan that was performed with a [<sup>137</sup>Cs] point source prior to the emission scans.

The radiotracer [<sup>15</sup>O]-water was used to measure rCBF (United States Pharmacopeia and The National Formulary 2006). For the [<sup>15</sup>O]-water scan, dynamic scanning began immediately upon a 25 mCi ±10% bolus radiotracer injection and lasted for three minutes. The radiotracer [<sup>11</sup>C]-3-amino-4-(2-dimethylaminomethyl-phenylsulfanyl)-enzonitrile ([<sup>11</sup>C]-DASB) was used to measure SERT and was synthesized as previously described (Wilson et al., 2002). For the [<sup>11</sup>C]-DASB scan, dynamic scanning began immediately upon a 20 mCi ±10% radiotracer injection and lasted for ninety minutes. [<sup>11</sup>C]-PiB was used to measure beta-amyloid deposition and was synthesized as previously described (Klunk et al., 2004). For the [<sup>11</sup>C]-PiB scan, dynamic scanning with the radiotracer N-methyl-[<sup>11</sup>C]2-(4'-methylaminophenyl)-6-hydroxybenzothiazole began immediately upon a 15 mCi ±10% radiotracer injection and lasted for ninety minutes. The cerebellum was used for the input function for [<sup>11</sup>C]-DASB and [<sup>11</sup>C]-PiB, as will be described.



The images for each radiotracer were reconstructed separately using the iterative ordered subset expectation maximization (OS-EM) algorithm (with 6 iterations and 16 subsets), with correction for radioactive decay, dead time, attenuation, scatter and randoms (Rahmim et al., 2005). Each PET scan was obtained in list mode then re-binned into frames, as defined below. The reconstructed image space consisted of cubic voxels, each 1.22 mm in size, and spanning dimensions of 256 (left-to-right) by 256 (nasion-to-inion) by 207 (neck-to-cranium). The final spatial resolution is expected to be less than 2.5 mm full width at half-maximum (FWHM) in three directions (Sossi et al., 2005). For the [<sup>15</sup>O]-water scans, a 60-sec frame was reconstructed, beginning 30 seconds after radiotracer administration, to allow time for the radiotracer to reach the brain (Raichle et al., 1983, Herscovich et al., 1983). The relationship between radioactivity counts in brain 30 seconds after radiotracer administration and rCBF is almost linear, and thus the PET image provides a measure that reflects relative rCBF. For the [<sup>11</sup>C]-DASB and [<sup>11</sup>C]-PiB scans, the ninety minute list mode data were binned into thirty frames (four 15 seconds, four 30 seconds, three 1 minute, two 2 minute, five 4 minute, and twelve 5 minute frames).

### MR Image Processing and Analysis

**Voxel-based Morphometry (VBM)**—VBM analysis was performed to evaluate differences in grey matter volumes between groups using Statistical Parametric Mapping, 8 (SPM8; Institute of Neurology, London) and MATLAB 7.10 (MathWorks, Natick, Massachusetts). The pre-processing involved the following steps: 1) MPRAGE images were manually aligned to the anterior commissure. 2) Images were segmented into grey matter, white matter, and cerebrospinal fluid using the unified segmentation model (Ashburner et al., 2005) 3) Nonlinear deformations to a grey matter template generated through iterative registration of individual grey matter images to a group average were estimated using the “Diffeomorphic Anatomical Registration Through Exponentiated Lie Algebra” (DARTEL) algorithm (Ashburner 2007) 4) A nonlinear transformation was estimated for the grey matter template, generated in the previous step, to normalize to Montreal Neurological Institute (MNI) space. 5) Individual grey matter images were normalized to MNI space using deformations estimated in steps 4 and 5, modulated to preserve tissue volumes, and smoothed with an isotropic Gaussian kernel (3mm FWHM for all directions). Statistical analyses were performed in SPM8 using the smoothed, modulated (tissue volume), and normalized grey matter images. To correct for individual differences in total brain volume, grey matter images were normalized (proportional scaling) using total intracranial volume computed for each subject in SPM8. A two-sample t-test was performed to evaluate between-group (MCI/control) differences in regional grey matter volumes.

### PET Image Processing and Analysis

**Tracer Kinetic Modelling and Parametric Imaging Methods**—For [<sup>11</sup>C]-DASB, parametric images of distribution volume ratio (DVR) and transport rate constant ratio (R<sub>1</sub>) were generated by using the simplified reference tissue model (SRTM) and linear regression with a spatial constraint parametric imaging algorithm (Zhou et al., 2003). The cerebellar (region of interest (ROI) time activity curve was used for the input function. As shown by Parsey et al (2006), the optimal cerebellar reference region for [<sup>11</sup>C]-DASB, includes the cerebellar hemisphere grey matter, not the white matter or vermis that may include SERT

specific binding. The delineation of the cerebellar reference region as defined by Parsey et al (2006) was performed to minimize the inclusion of SERT specific binding in the reference region by limiting the ROI to the cerebellar hemisphere grey matter. [ $^{11}\text{C}$ ]-PiB was analyzed using the same SRTM method using the cerebellum as the input function that has been validated against arterial blood sampling (Zhou et al., 2003, Price et al., 2005). For [ $^{15}\text{O}$ ]-water, to correct for individual differences in radiotracer concentrations and global blood flow, the 60-sec frames were normalized to the whole brain grey matter blood flow based on a mask generated using voxel based morphometry.

**Voxel-wise PET Analyses**—The pre-processing and voxel-wise statistical analyses of the parametric [ $^{11}\text{C}$ ]-DASB DVR images and the [ $^{15}\text{O}$ ]-water images were performed also with SPM8. PET to PET and MR to PET co-registration was performed using the normalized mutual information algorithm. The images were spatially normalized into standard 3-dimensional space relative to the anterior commissure using the DARTEL template that was generated as described above. For the voxel-wise analyses, the parametric [ $^{11}\text{C}$ ]-DASB DVR images and [ $^{15}\text{O}$ ]-water images were smoothed with an isotropic Gaussian kernel (3mm FWHM). A between-subjects comparison of the [ $^{11}\text{C}$ ]-DASB DVR images and [ $^{15}\text{O}$ ]-water images was performed using the flexible factorial option (one-way ANOVA) to evaluate the differences between MCIs and controls. For the statistical analyses, the results reported are the peak voxels within anatomical regions that belong to the same cluster, as represented on different rows of the tables. Brain locations are reported as x, y, z coordinates in MNI space with approximate Brodmann areas (BA) identified by mathematical transformation of MNI coordinates into Talairach space (<http://www.mrc-cbu.cam.ac.uk/Imaging/>).

For the [ $^{11}\text{C}$ ]-DASB analyses, the between-group comparisons reported were significant at a cluster-level FDR corrected value of  $p < 0.001$ . The peak voxels within the clusters are reported at an uncorrected peak voxel-value of  $p < 0.001$  (Height threshold  $p=0.01$  and extent threshold ( $k$ ) =50 voxels). For the [ $^{15}\text{O}$ ]-water analyses, the between-group comparisons were not significant at a cluster-level FDR corrected value of  $p < 0.05$ . The peak voxels within the clusters are reported at an uncorrected peak voxel-value of  $p < 0.001$  (Height threshold  $p=0.01$  and extent threshold ( $k$ ) =50 voxels). Then, one-sample t-tests were performed within each group with cognitive variables as co-variates (CVLT and BVMT-R) to determine whether the co-variates contributed significant variance to SERT in controls and MCI. The correlations between SERT and the memory measures are reported at a cluster-level FDR corrected value of  $p < 0.001$ . The peak voxels within the clusters are reported at an uncorrected peak voxel-value of  $p < 0.001$  (Height threshold  $p=0.01$  and extent threshold ( $k$ ) =50 voxels).

To determine the magnitude of the between group differences in SERT, representative voxel values were extracted from the SPM8 analysis using the eigenvariate feature. The medial raphe nucleus (MRN) and dorsal raphe nucleus (DRN) were identified on the sagittal plane of the DARTEL-normalized MPRAGE using anatomical landmarks (Kranz et al., 2012). The MRN and DRN ROIs were drawn on the individual MRI scan for each subject as a standard sphere of 3mm in diameter and placed between the superior and inferior colliculus starting medially and extending laterally. The ROIs were visually inspected on all participants' MRI and PET scans to confirm the correct anatomical localization.



**Exploratory Factor Analysis**—To determine associations among SERT ROIs, an exploratory factor analysis was performed with SERT ROIs for the MCIs and controls. SERT ROIs were defined using FreeSurfer (version 5.1; <http://surfer.nmr.mgh.harvard.edu/>). First, each individual's MPRAGE was submitted to the FreeSurfer processing pipeline to create subject specific labels for each ROI. Then, each ROI was converted to a volumetric mask using the `mri_annotation2label` and `mri_label2vol` commands that are part of the FreeSurfer package. Finally, these volumetric ROI masks were overlaid onto parametric SERT images that were previously co-registered using SPM8 to the subject's native MR space. Descriptive SERT statistics (mean, maximum, minimum, and standard deviation) for the voxels within each region were generated with a script composed of SPM8 functions. The raphe nuclei ROIs are not available in FreeSurfer and were manually drawn, as described above. The same methods were used to define ROIs for [<sup>11</sup>C]-PiB to measure regional beta-amyloid deposition.

SERT ROIs for each participant were averaged across the right and left hemispheres and entered into an exploratory factor analysis using *minres* factor extraction and iterative bootstrapping to estimate confidence intervals for model parameters (Harman et al., 1966). Factor analysis was completed using the *fa* function in the *psych* toolbox in the *R* statistical package (Revelle, 2015, R Core Team, 2015). Though the sample size is small, reliable factor solutions can be found in datasets with high communalities, and bootstrapped confidence intervals will aid in assessment of the reliability of the final factor solution (MacCallum et al., 2001). Since the SERT ROIs may be highly correlated, an oblique factor rotation (oblimin) was applied to the factor solution, as this will permit factors to correlate freely. Both scree plot inspection and parallel analysis were used to identify the number of factors to extract. ROIs with loadings less than 0.4 onto any factor, or with loadings greater than 0.4 on more than one factor, were removed from the analysis. Given the small number of observations (subjects) relative to the ROIs (variables), an initial model was fit to identify the pattern of factor loadings, and then a subsequent model was fit that only retained the highest-loading ROIs from the previous model (loadings  $\geq 0.7$ ). Factor scores for each participant were generated using the regression method, and these scores were subsequently compared between groups (MCI/ control) using paired t-tests with unequal variance.

## RESULTS

### Demographic, Clinical and Neuropsychological Variables (Table 1)

The MCI and control groups did not differ significantly in age ( $F(1,55)=1.13$ ,  $p > 0.05$ ), sex distribution ( $\chi^2(1) = 0.07$ ;  $p > 0.05$ ) or years of education ( $F(1,55)=0.72$ ;  $p > 0.05$ ). One of the controls and two of the MCI participants were left handed. The control group included 18 white, 8 African American, 1 Asian American and 1 Hispanic participant. The MCI group included 23 white and 5 African American participants. None of the participants had ever taken an antidepressant or other psychotropic drugs. As expected, the MCIs performed significantly worse than controls on the cognitive measures, including the MMSE ( $F(1,55)=6.1$ ;  $p < 0.05$ ), CVLT sum of the first five trials ( $F(1,55)=27.6$ ;  $p < 0.001$ ) and the BVMT-R-sum of the three learning trials ( $F(1,55)=20.6$ ;  $p < 0.001$ ). The MCIs had a significantly higher NPI score relative to the controls ( $F(1,55)=9.30$ ;  $p < 0.005$ ), although

the NPI scores were within a mild range of symptoms. All of the MCIs underwent PET beta-amyloid imaging with the radiotracer [11C]-PiB and demonstrated a distribution volume ratio that is associated with cognitive decline; 1.2 or higher for anterior (anterior cingulate or middle frontal cortex) and/or posterior cortical regions (superior temporal cortex, precuneus or posterior cingulate; data not shown; Resnick et al., 2010). In addition, all of the MCIs performed at least one standard deviation below the normative value on either the CVLT or the BVM-T-R or both (data not shown). Thus, based on the beta-amyloid imaging and cognitive performance, this MCI sample is likely to demonstrate future cognitive decline.

### Voxel-wise analysis of Grey Matter Volumes and rCBF

There were no significant differences in grey matter volumes and rCBF in MCI compared to controls, at the significance threshold reported for the SERT data (cluster-level FDR corrected value of  $p = 0.001$ ). The VBM and rCBF results of the between group comparisons that are reported were also not significant at a cluster-level FDR corrected value of  $p = 0.05$ . The peak voxels within the clusters are reported at an uncorrected peak voxel-value of  $p < 0.05$  (Height threshold  $p = 0.05$  and extent threshold ( $k = 50$  voxels). At this less stringent peak probability level, lower grey matter volumes and rCBF in MCI compared to controls was localized to temporal and parietal regions. Lower grey matter volumes in MCI compared to controls were observed in bilateral middle and inferior temporal gyri and right fusiform gyrus. rCBF was lower in MCI than controls in the left middle temporal gyrus, left posterior cingulate gyrus, and left precuneus. Thus, widespread lower cortical SERT in MCI compared to controls that will be reported below is more extensive than the lower grey matter or rCBF that was localized to temporal and parietal cortices.

### Voxel-wise analyses of SERT (Figure 1 and Figure 2a, Table 2; Supplemental Table s-1)

Significantly lower SERT in the MCIs compared to controls was observed in the following brain regions: right superior (BA 10), medial (BA 9), middle (left BA 10/right BA 46) and right inferior frontal gyri (BA 46), right pre-central gyrus (BA 6), insula (BA 13), anterior cingulate gyrus (BA 24/right BA 32), superior (BA 38, left BA 41/ right BA 39), middle (BA 21, left BA 22 and left BA 39) and inferior (BA 20) temporal gyri, uncus (left BA 38/right BA 36), amygdala, left hippocampus, uncus (left BA 38, right BA 36), parahippocampal gyrus (left BA 36, right BA 28, BA 30, BA 34, BA 35, BA 37), left post-central gyrus (BA 43), precuneus (BA 31), posterior cingulate gyrus (BA 23, BA 30, right BA 31), fusiform gyrus (BA 20, BA 37), lingual gyrus (BA 18), left middle occipital gyrus (BA 19), cuneus (BA 17, BA 18, BA 30), caudate, left putamen, claustrum, left medial and lateral globus pallidus and thalamus (pulvinar; all regions bilateral unless noted otherwise). There were no significant regions of higher SERT in the MCIs compared to controls. The magnitude of reduction of SERT in MCI compared to controls ranged from 10–38%. The summed parametric images from the MCIs and the control subjects are shown in Figure 1. Means and standard deviations for representative regions are shown in Table 2. The voxel-wise results of the between-group differences in SERT are shown in Figure 2a. The SPM T-maps for these and the correlation analyses are superimposed on a 3D rendering of the International Consortium for Brain Mapping (ICBM) 152 non-linear atlas that represents MPRAGE MRI images averaged over 153 healthy control participants (2009 version; Fonov et al., 2009, 2011).

### Correlations between SERT and the CVLT and BVMT-R (Figure 2b and 2c, Supplemental Table s-2a,b)

For both the CVLT and BVMT-R, the correlations with SERT were positive (higher SERT was associated with better performance). The correlations were only observed in the MCIs, not the controls. The regions that showed significant correlations for both tests were consistent with the regions that showed lower SERT in the MCIs. For the CVLT, in the MCIs, significant positive correlations were observed in the superior (right BA6, left BA 8), left middle (BA9) and left inferior frontal gyri (BA47), anterior cingulate gyrus (bilateral BA 24 and left BA 32), left inferior temporal gyrus (BA 20, lBA 37), uncus (BA 28), parahippocampal gyrus (BA 34, BA 35), amygdala, right superior parietal lobule (BA 7), left precuneus (lBA 7), left posterior cingulate (BA 30, BA 31), left fusiform gyrus (BA 37), left cuneus (BA 19), left caudate, bilateral putamen and left thalamus.

For the BVMT-R, in the MCIs, significant positive correlations were observed in the superior (left BA 6 and left BA 9, right BA10), medial (left BA 6 and left BA9, bilateral BA 10) and inferior frontal gyri (left BA 9/right BA 45), left insula (BA 13), left anterior cingulate gyrus (BA 32), superior (BA 22, right BA 38) and middle (BA 21) temporal gyri, left parahippocampal gyrus (BA 28), left inferior parietal lobule (BA 40), left precuneus (BA 31), left lingual gyrus (BA 18), and left thalamus (medial-dorsal nucleus). The voxel-wise results of the correlations between SERT and the CVLT and SERT and the BVMT-R are shown in Figures 2b and 2c, respectively.

### Exploratory factor analysis (Table 3)

A two-factor solution was indicated by the parallel analysis and inspection of the scree plots. Eight regions of interest (superior, middle, and inferior temporal gyri, fusiform gyrus, isthmus of the cingulate gyrus, rostral anterior cingulate gyrus, insula, and parahippocampal gyrus) loaded greater than 0.4 on more than one factor (no greater than 0.63 on any factor). Thus, these ROIs were excluded, and the analysis was re-estimated. Then, all ROIs with primary loadings below 0.7 (including medial and lateral orbitofrontal, transverse temporal, pericalcarine, and caudal anterior cingulate ROIs, which all loaded onto the first factor), were removed and the model was re-fitted. The resulting model yielded one ultra-Heywood case (ventral diencephalon, loading = 1.03) in the second factor, which was driven by the small sample size (52 observations for 30 ROIs). The lowest-loading items were iteratively removed from the second factor (entorhinal cortex, temporal pole, thalamus, and accumbens area; all items loading > 0.72 when removed) until a model was reached with no Heywood cases. The final model yielded good model fit (root mean square residual  $[RMSR] = 0.04$ ), moderately high factor inter-correlations ( $r = 0.62$  [0.44–0.77]), and a simple structure. Bootstrapped confidence intervals provide a non-parametric measure of the significance and reliability of each factor loading and aid in assessment of the reliability of the final factor solution. As observed in the data, the confidence intervals derived from bootstrapping show that factor loadings for each variable are significant (i.e. they do not include 0) and are within acceptable ranges for meaningful factor loadings (i.e. confidence intervals as well as factor loadings are greater than 0.3 which is the minimal factor loading for significance as recommended by Hair et al., 1998, Field, 2013, and Tabachnick and Fidell, 2014).

The first factor accounted for 61% of the variance in SERT, included loadings from mainly frontal, parietal and occipital regions (including association cortices, as well as sensory and motor cortices), and was labeled the Cortical SERT factor. Cortical SERT factor scores were significantly different between MCI and control groups ( $\text{mean}_{\text{controls}} = 0.256$ ,  $\text{mean}_{\text{mci}} = -0.276$ ,  $t = 2.015$ ,  $df = 52$ ,  $p = 0.049$ ). The second factor explained 22% of the variance in the model, included loadings from a number of limbic (amygdala, hippocampus) and subcortical (caudate, putamen, pallidum, ventral diencephalon and dorsal Raphe) regions, and was identified as the Subcortical SERT factor. Subcortical SERT Factor scores were also significantly different between groups ( $\text{mean}_{\text{controls}} = 0.338$ ,  $\text{mean}_{\text{mci}} = -0.364$ ,  $t = -2.775$ ,  $df = 51$ ,  $p = 0.008$ ). The t-tests were replicated after re-introducing the ROIs with primary loadings less than 0.7. This factor model yielded similar results.

## Discussion

As hypothesized, lower SERT was observed in MCIs relative to healthy controls in the cortical (including the heteromodal association cortices of the frontal, temporal, and parietal lobes), limbic regions (amygdala, hippocampus) and peri-limbic regions (including anterior cingulate and insula) and the raphe nuclei. In addition, lower SERT was observed in the basal ganglia, thalamus and sensory and motor cortices, which are relatively spared in AD neuropathology and glucose metabolic deficits (Arnold et al., 1991, Smith et al., 1992). The regions that had diminished SERT in MCI included those regions with relatively high SERT in the normal, healthy human brain, including the anterior cingulate gyrus, insula, caudate, putamen and pulvinar (Steinbusch, 1981, Varnäs et al., 2004). The magnitude of lower SERT in MCI compared to controls ranged from 10–19% in cortical regions and the raphe nuclei and 10%–38% in striatum and thalamus (to the greatest extent in the caudate). The results of the factor analysis were consistent with the voxel-wise results. The factor analysis also showed significantly lower SERT in MCIs than controls through the identification of separate Cortical and Subcortical SERT factors. Interestingly, the Cortical factor explained more of the variance in SERT than the Subcortical factor. The cortical factor included association cortices, as well as primary sensory and motor areas. Both types of cortical regions were lower in MCI compared to controls in the voxel-wise analyses. Thus, the results of the factor analysis demonstrated lower SERT in MCI than controls using an independent analysis method.

The widespread loss of SERT in cortical regions in MCI is consistent with lower, widespread cortical 5-HT<sub>2A</sub> receptors as observed in PET studies in MCI (Hasselbalch et al., 2008). While both higher and lower cortical 5-HT<sub>1A</sub> receptors have been reported in MCI, lower SERT could be associated with a compensatory up-regulation of 5-HT<sub>1A</sub> receptors or with a secondary down-regulation of 5-HT<sub>1A</sub> receptors (Truchot et al., 2008, Kepe et al., 2006). The observation of lower SERT in MCI compared to controls is complementary to the results of serotonin receptor studies and suggests that lower 5-HT<sub>2A</sub> and 5-HT<sub>1A</sub> receptors may be associated, in part, with deficits in serotonergic function, as well as in other neurotransmitters associated with these receptor subtypes (e.g. acetylcholine; Quirion et al., 1985, 1987). The limited SERT data in AD has shown lower SERT in more localized regions as compared to the present study in MCI (Ouichi et al., 2009, Marner et al., 2012). The present study differs from these studies in several

methodological respects that may affect the comparison across studies, including a larger sample size, use of a high resolution PET scanner and confirmation of PET beta-amyloid status in the MCIs.

The reduction in SERT is observed in temporal and parietal cortices, as well as cortical and sub-cortical regions, and is more extensive than grey matter atrophy or reduced rCBF that is observed in temporal and parietal regions. The grey matter atrophy and reduced rCBF in temporal and parietal cortices of MCI participants relative to healthy controls is consistent with reports in the literature (as reviewed by Wolf et al., 2003). While the volumetric and rCBF deficits may not be as great in magnitude or extent as might be expected, the MCIs were relatively young and carefully screened for medical comorbidities that might have a greater impact on brain structure and function. As the MCIs demonstrated levels of beta-amyloid deposition and cognitive deficits in a range associated with cognitive decline. Thus, this is a group that is likely to show cognitive decline over time. Lower SERT was correlated with worse performance in tests of auditory-verbal and visual-spatial memory, to a greater extent in the MCIs than controls. These correlations are consistent with previous studies that have shown deficits in verbal (human) and visual-spatial memory (human and animal) with lesions of or damage to the serotonin system that decreased SERT (Cabeza and Nyberg, 2000, Cowen and Sherwood, 2013).

There are several limitations to the present study. First, arterial blood was not obtained for the input function for quantification of [ $^{11}\text{C}$ ]-DASB, but rather a reference region approach was used. The cerebellar grey matter was used as the reference region and was carefully delineated to include grey matter and to exclude specific binding of SERT in the cerebellar white matter, an approach that has been validated against arterial blood sampling (Parsey et al., 2006). Nonetheless, the possibility cannot be excluded that the cerebellar input function could cause an underestimation of the binding across groups. There are some reports that the outcome measure chosen for [ $^{11}\text{C}$ ]-DASB could determine detection of between-group differences between patients and controls (Miller et al., 2016). This was observed in a study in patients with bipolar disorder that employed an arterial input function, as well as determination of the plasma free fraction (Fp), neither of which was obtained in the present study. There is no *a priori* reason to expect Fp to differ between MCI and control groups, as all participants underwent careful medical screening, were medically stable and had no psychotropic drug use, as confirmed by toxicology screening. The observations by Miller et al (2016) underscore the importance of reference-free mathematical models (e.g. Ogden et al., 2015) to address the problem of specific binding in a reference region. Secondly, partial volume correction was not employed as methods are still being validated for the HRRT scanner used in this study and have not yet been adapted for voxel-wise analysis. Theoretically, partial volume correction should be less necessary for the HRRT because of its higher spatial resolution (approximately 2.5 mm FWHM). The possibility that SERT loss in MCI is secondary to gray matter volume loss or reductions in brain function is addressed to some extent by the volumetric and rCBF results that show more localized and less statistically robust grey matter volume loss and rCBF deficits than SERT loss.

The loss of SERT in MCI may have a substantial impact on brain function and behavior given the widespread distribution of SERT in the brain and the evidence that serotonin

modulates other neurotransmitters (glutamate, norepinephrine, dopamine and acetylcholine) implicated in AD and potentially MCI (Golembiowska and Dziubina, 2000, Invernizzi, et al., 1997, Lucas et al., 2000, Mateo et al., 2000, Hilgert et al., 2000). The regions of cortical SERT loss overlap with the regions that show lower cerebral glucose metabolism after acute citalopram administration, including the heteromodal association cortices (Smith et al., 2002, 2009). The critical modulatory role of serotonin is underscored by the dense serotonin innervation throughout the central nervous system and the observation that in the rat brain, every cell in the cortex is in close proximity to a serotonin containing neuron (Molliver, 1987). Serotonin degeneration may impair the function of serotonin signaling pathways that activate cyclic AMP response element binding protein (CREB) and up-regulate expression of brain derived neurotrophic factor (BDNF; as reviewed by Mattson et al., 2004). The inability to activate these pathways may affect synaptic plasticity and result in synaptic dysfunction and neuronal death.

Medications that target the serotonin system are widely used in MCI and AD for the treatment of neuropsychiatric symptoms (e.g. antidepressant and antipsychotic medications; Zhu et al., 2011). The substantially lower SERT in MCI observed in the present study, suggests that the serotonin system may represent an important target for prevention and treatment. Treatments that target the post-synaptic receptors (5-HT<sub>4</sub> agonists, 5-HT<sub>6</sub> antagonists) that may not be affected as severely as SERT and may modulate the function of other neurotransmitters may be more effective than selective serotonin reuptake inhibitors (as reviewed by Meneses, 2013). In fact, serotonergic compounds are the only therapeutic agents with preclinical evidence of blocking amyloid precursor protein processing and beta-amyloid deposition, providing neuroprotection, supporting synaptic plasticity and improving both cognitive deficits and neuropsychiatric symptoms (e.g. selective 5-HT reuptake inhibitors, 5-HT<sub>4</sub> agonists and 5-HT<sub>6</sub> antagonists; Mattson, et al., 2004, Tucker et al., 2006, Nelson et al., 2007). Serotonergic agents could be used, potentially, to prevent cognitive decline and the emergence of neuropsychiatric symptoms. While there are compelling clinical data to support the serotonin system as a treatment target, further investigation is needed to understand the role of serotonin degeneration with respect to whether it is a downstream effect of AD pathology or plays a causative role.

In summary, the results of the present study demonstrate lower SERT in cortical, striatal, thalamic and limbic regions in MCIs relative to controls. Grey matter atrophy and reductions in regional cerebral blood flow in mild cognitive impairment compared to controls was more localized and less statistically robust than the reductions in SERT. The reduction in SERT is associated with greater impairment in auditory-verbal and visual-spatial memory in MCI. Studies are in progress to determine whether serotonin degeneration may be involved in the transition from MCI to dementia and to relate serotonin degeneration to other aspects of AD neuropathology (e.g. beta-amyloid and tau).

## Supplementary Material

Refer to Web version on PubMed Central for supplementary material.



## Acknowledgments

The authors gratefully acknowledge Karen Edmonds; Bineyam Gebrewold; Michael Hans, Jose Leon and David J. Clough for their invaluable contribution to the acquisition of the PET data, Terri Brawner, Ivana Kusevic, and Kathy Kahl for their invaluable contribution to the acquisition of the MR data.

Funding/Support: This study was supported by: National Institute of Health: AG038893, AG041633, and UL1 TR 001079. Conflict of Interest Disclosures: None reported.

## References

- Arnold SE, Hyman BT, Flory J, Damasio AR, Van Hoesen GW. The topographical and neuroanatomical distribution of neurofibrillary tangles and neuritic plaques in the cerebral cortex of patients with Alzheimer's disease. *Cereb Cortex*. 1991; 1(1):103–16. [PubMed: 1822725]
- Ashburner J, Friston KJ. Unified segmentation. *Neuroimage*. 2005; 26:839–851. [PubMed: 15955494]
- Ashburner J. A fast diffeomorphic image registration algorithm. *Neuroimage*. 2007; 38:95–113. [PubMed: 17761438]
- Azmitia E, Nixon R. Dystrophic serotonergic axons in neurodegenerative diseases. *Brain Res*. 2008; 1217:185–94. [PubMed: 18502405]
- Baker GB, Reynolds GP. Biogenic amines and their metabolites in Alzheimer's disease: noradrenaline, 5-hydroxytryptamine and 5-hydroxyindole-3-acetic acid depleted in hippocampus but not in substantia innominata. *Neurosci Lett*. 1989; 100(1–3):335–9. [PubMed: 2474777]
- Benedict, RHB. Brief Visuospatial Memory Test – Revised: Professional manual. Odessa, FL: Psychological Assessment Resources, Inc; 1997.
- Blakely RD, Ramamoorthy S, Schroeter S, Qian Y, Apparsundaram S, Galli A, DeFelice LJ. Regulated Phosphorylation and Trafficking of Antidepressant-Sensitive Serotonin Transporter Proteins. *Biol Psychiatry*. 1998; 44:169–178. [PubMed: 9693389]
- Blin J, Baron JC, Dubois B, Cruzel C, Fiorelli M, Attar-Levy D, Pillon B, Fournier D, Vidailhet M, Agid Y. Loss of brain 5-HT<sub>2</sub> receptors in Alzheimer's disease. In vivo assessment with positron emission tomography and [18F]setoperone. *Brain*. 1993; 116(Pt 3):497–510. [PubMed: 8513389]
- Bowen DM, Allen SJ, Benton JS, Goodhardt MJ, Haan EA, Palmer AM, Sims NR, Smith CC, Spillane JA, Esiri MM, Neary D, Snowden JS, Wilcock GK, Davison AN. Biochemical assessment of serotonergic and cholinergic dysfunction and cerebral atrophy in Alzheimer's disease. *Journal of Neurochemistry*. 1983; 41:266–272. [PubMed: 6306169]
- Bowen DM, White P, Spillane JA, Goodhardt MJ, Curzon G, Iwagoff P, Meier-Ruge W, Davison AN. Accelerated aging or selective neuronal loss as an important cause of dementia? *Lancet*. 1979; 1(8106):11–14. [PubMed: 83462]
- Cabeza R, Nyberg L. Imaging cognition II: An empirical review of 275 PET and fMRI studies. *J Cogn Neurosci*. 2000; 12:1–47.
- Cowen P, Sherwood AC. The role of serotonin in cognitive function: evidence from recent studies and implications for understanding depression. *J Psychopharmacol*. 2013; 27(7):575–83. [PubMed: 23535352]
- Cross A, Crow T, Ferrier I, Johnson J. The selectivity of the reduction of serotonin S<sub>2</sub> receptors in Alzheimer-type dementia. *Neurobiol Aging*. 1986; 7(1):3–7. [PubMed: 2869422]
- Curcio C, Kemper T. Nucleus raphe dorsalis in dementia of the Alzheimer type: Neurofibrillary changes and neuronal packing density. *Journal of Neuropathology and Experimental Neurology*. 1984; 43(4):359–368.
- Cummings JL, Mega M, Gray K, Rosenberg-Thompson S, Carusi DA, Gornbein J. The Neuropsychiatric Inventory: Comprehensive Assessment of Psychopathology in Dementia. *Neurology*. 1994; 44:2308–2314. [PubMed: 7991117]
- D'Amato R, Zweig R, Whitehouse P, et al. Aminergic systems in Alzheimer's disease and Parkinson's disease. *Annals of Neurology*. 1983; 22:229–236.
- Delis DC, Freeland J, Kramer JH, et al. Integrating clinical assessment with cognitive neuroscience: construct validation of the California Verbal Learning Test. *J Consult Clin Psychol*. 1988; 56:123–130. [PubMed: 3346437]

- Elliott MS, Ballard CG, Kalaria RN, Perry R, Hortobágyi T, Francis PT. Increased binding to 5-HT<sub>1A</sub> and 5-HT<sub>2A</sub> receptors is associated with large vessel infarction and relative preservation of cognition. *Brain*. 2009; 132(Pt 7):1858–65. [PubMed: 19433439]
- Field, A. *Discovering Statistics using SPSS*. 4. London: SAGE; 2013.
- First, M., Spitzer, R., Gibbon, M., Williams, J. *Structured clinical interview for DSM-IV axis 1 disorders-patient edition (SCID-I/P)*. New York: New York Psychiatric Institute; 1995.
- Folstein M, Folstein S, McHugh P. Mini-mental state. *Journal of Psychiatric Research*. 1976; 12:189–198.
- Fonov VS, Evans AC, Botteron K, Almli CR, McKinstry RC, Collins DLBDCG. Unbiased average age-appropriate atlases for pediatric studies. *Neuroimage*. 2011; 54(1):313–327. [PubMed: 20656036]
- Fonov VS, Evans AC, McKinstry RC, Almli CR, Collins DL. Unbiased nonlinear average age-appropriate brain templates from birth to adulthood. *Neuroimage*. 2009; 47(1):S102.
- Golembiowska K, Dziubina A. Effect of acute and chronic administration of citalopram on glutamate and aspartate release in the rat prefrontal cortex. *Polish J Pharm*. 2000; 52(6):441–8.
- Hair, JF., Jr, Anderson, RE., Tatham, RL., Black, WC. *Multivariate Data Analysis*. 5. Upper Saddle River, NJ: Prentice Hall; 1998.
- Harman H, Jones W. Factor analysis by minimizing residuals (minres). *Psychometrika*. 1966; 31(3): 351–368. [PubMed: 5221131]
- Hasselbalch SG, Madsen K, Svarer C, Pinborg LH, Holm S, Paulson OB, Waldemar G, Knudsen GM. Reduced 5-HT<sub>2A</sub> receptor binding in patients with mild cognitive impairment. *Neurobiology of Aging*. 2008; 29(12):1830–8. [PubMed: 17544547]
- Herscovitch P, Markham J, Raichle ME. Brain blood flow measured with intravenous H<sub>2</sub>(<sup>15</sup>O). I. Theory and error analysis. *J Nucl Med*. 1983; 24(9):782–9. [PubMed: 6604139]
- Hilgert M, Buchholzer M, Jeltsch H, Kelche C, Cassel JC, Klein J. Serotonergic modulation of hippocampal acetylcholine release after long-term neuronal grafting. *Neurorep*. 2000; 11:3063–3065.
- Hirao K, Smith GS. Positron Emission Tomography Molecular Imaging in Late-Life Depression. *J Geriatr Psych Neurol*. 2014; 27(1):13–23.
- Invernizzi R, Velasco C, Bramante M, Longo A, Samanin R. Effect of 5-HT<sub>1A</sub> receptor antagonists on citalopram-induced increase in extracellular serotonin in the frontal cortex, striatum and dorsal hippocampus. *Neuropharm*. 1997; 36:467–473.
- Kepe V, Barrio JR, Huang SC, Ercoli L, Siddarth P, Shoghi-Jadid K, Cole GM, Satyamurthy N, Cummings JL, Small GW, Phelps ME. Serotonin 1A receptors in the living brain of Alzheimer's disease patients. *Proc Nat Acad Sci USA*. 2006; 103(3):702. [PubMed: 16407119]
- Kranz GS, Hahn A, Savli M, Lanzenberger R. Challenges in the differentiation of midbrain raphe nuclei in neuroimaging research. *Proc Natl Acad Sci U S A*. 2012; 109(29):E2000. [PubMed: 22711836]
- Blunk WE, Engler H, Nordberg A, Wang Y, Blomqvist G, Holt DP, Bergström M, Savitcheva I, Huang GF, Estrada S, Ausén B, Debnath ML, Barletta J, Price JC, Sandell J, Lopresti BJ, Wall A, Koivisto P, Antoni G, Mathis CA, Långström B. Imaging brain amyloid in Alzheimer's disease with Pittsburgh Compound-B. *Ann Neurol*. 2004; 55(3):306–19. [PubMed: 14991808]
- Lancot KL, Hussey DF, Herrmann N, Black SE, Rusjan PM, Wilson AA, Houle S, Kozloff N, Verhoeff NP, Kapur S. A Positron Emission Tomography Study of 5-Hydroxytryptamine-1A Receptors in Alzheimer Disease. *Am J Geriatr Psych*. 2007; 15(10):888–98.
- Liu Y, Yoo MJ, Savonenko A, Stirling W, Price DL, Borchelt DR, Mamounas L, Lyons WE, Blue ME, Lee MK. Amyloid pathology is associated with progressive monoaminergic neurodegeneration in a transgenic mouse model of Alzheimer's disease. *J Neurosci*. 2008; 28(51):13805–14. [PubMed: 19091971]
- Lucas G, De Deurwaerdere P, Porras G, Spampinato U. Endogenous serotonin enhances the release of dopamine in the striatum only when nigro-striatal dopaminergic transmission is activated. *Neuropharmacol*. 2000; 39(11):1984–1995.
- MacCallum R, Widaman K, Preacher K, Hong S. Sample size in factor analysis: The role of model error. *Multivariate Behavioral Resesarch*. 2001; 36(4):611–637.

- Mann DM, Yates PO. Serotonin nerve cells in Alzheimer's disease. *J Neurol Neurosurg Psychiatr.* 1983; 46:96–98.
- Marcusson JO, Alafuzoff I, Bäckström IT, Ericson E, Gottfries CG, Winblad B5-Hydroxytryptaminesensitive [3H]imipramine binding of protein nature in the human brain. II. Effect of normal aging and dementia disorders. *Brain Res.* 1987; 425(1):137–45. [PubMed: 3427415]
- Marner L, Frokjaer VG, Kalbitzer J, Lehel S, Madsen K, Baaré WF, Knudsen GM, Hasselbalch SG. Loss of serotonin 2A receptors exceeds loss of serotonergic projections in early Alzheimer's disease: a combined [11C]DASB and [18F]altanserin-PET study. *Neurobiol Aging.* 2012; 33(3): 479–87. [PubMed: 20510480]
- Mateo Y, Ruiz-Ortega JA, Pineda J, Ugedo L, Meana JJ. Inhibition of 5-hydroxytryptamine reuptake by the antidepressant citalopram in the locus coeruleus modulates the rat brain noradrenergic transmission in vivo. *Neuropharmacol.* 2000; 39(11):2036–2043.
- Mattson MP, Maudsley S, Martin B. BDNF and 5-HT: a dynamic duo in age-related neuronal plasticity and neurodegenerative disorders. *Trends Neurosci.* 2004; 27(10):589–94. [PubMed: 15374669]
- Meneses A. 5-HT systems: emergent targets for memory formation and memory alterations. *Rev Neurosci.* 2013; 24(6):629–64. [PubMed: 24259245]
- Miller JM, Everett BA, Oquendo MA, Ogden RT, Mann JJ, Parsey RV. Positron emission tomography quantification of serotonin transporter binding in medication-free bipolar disorder. *Synapse.* 2016; 70(1):24–32. [PubMed: 26426356]
- Molliver ME. Serotonergic neuronal systems: what their anatomic organization tells us about function. *J Clin Psychopharm.* 1987; 7(6 Suppl):3S–23S.
- Morris JC. The Clinical Dementia Rating (CDR): current version and scoring rules. *Neurol.* 1993; 43(11):2412–4.
- Nazarali A, Reynolds G. Monoamine neurotransmitters and their metabolites in brain regions in Alzheimer's disease: A postmortem study. *Cell Mol Biol.* 1992; 12(6):581–587.
- Nelson RL, Guo Z, Halagappa VM, Pearson M, Gray AJ, Matsuoka Y, Brown M, Martin B, Iyun T, Maudsley S, Clark RF, Mattson MP. Prophylactic treatment with paroxetine ameliorates behavioral deficits and retards the development of amyloid and tau pathologies in 3xTgAD mice. *Experimental Neurology.* 2007; 205(1):166–76. [PubMed: 17368447]
- Ouchi Y, Yoshikawa E, Futatsubashi M, Yagi S, Ueki T, Nakamura K. Altered brain serotonin transporter and associated glucose metabolism in Alzheimer disease. *J Nucl Med.* 2009; 50(8): 1260–6. [PubMed: 19617327]
- Ogden RT, Zanderigo F, Parsey RV. Estimation of in vivo nonspecific binding in positron emission tomography studies without requiring a reference region. *Neuroimage.* 2015; 108:234–242. [PubMed: 25542534]
- Quirion R, Richard J, Dam T. Evidence for the existence of serotonin type-2 receptors on cholinergic terminals in rat cortex. *Brain Res.* 1985; 333:345–349. [PubMed: 3995301]
- Quirion R, Richard J. Differential effects of selective lesions of cholinergic and dopaminergic neurons on serotonin-type 1 receptors in rat brain. *Synapse.* 1987; 1:124–130. [PubMed: 3145578]
- Palmer A, Stratmann G, Procter A, Bowen D. Possible neurotransmitter basis of behavioral changes in Alzheimer's Disease. *Ann Neurol.* 1988; 23:616–620. [PubMed: 2457353]
- Parsey RV, Kent JM, Oquendo MA, Richards MC, et al. Acute occupancy of brain serotonin transporter by Sertraline as measured by [<sup>11</sup>C]DASB and positron emission tomography. *Biol Psychiatr.* 2006; 59(9):821–8. [PubMed: 16213473]
- Price JC, Klunk WE, Lopresti BJ, Lu X, Hoge JA, Ziolkowski SK, Holt DP, Meltzer CC, DeKosky ST, Mathis CA. Kinetic modeling of amyloid binding in humans using PET imaging and Pittsburgh Compound-B. *J Cereb Blood Flow Metab.* 2005; 25(11):1528–47. [PubMed: 15944649]
- R Core Team. R: A language and environment for statistical computing. R Foundation for Statistical Computing; Vienna, Austria: 2015.
- Raichle ME, Martin WR, Herscovitch P, Mintun MA, Markham J. Brain blood flow measured with intravenous H<sub>2</sub>(<sup>15</sup>O). II. Implementation and validation. *J Nucl Med.* 1983; 24(9):790–8. [PubMed: 6604140]

- Rahmim A, Cheng JC, Blinder S, Camborde ML, Sossi V. Statistical dynamic image reconstruction in state-of-the-art high resolution PET. *Phys Med Biol*. 2005; 50:4887–4912. [PubMed: 16204879]
- Resnick SM, Sojkova J, Zhou Y, An Y, Ye W, Holt DP, et al. Longitudinal cognitive decline is associated with fibrillar amyloid-beta measured by [<sup>11</sup>C]PiB. *Neurology*. 2010; 74(10):807–815. [PubMed: 20147655]
- Revelle, W. *psych: Procedures for Personality and Psychological Research*. Northwestern University, Evanston; Illinois, USA: 2015.
- Rub U, Del Tredici K, Schultz C, Thal DR, Braak E, Braak H. The evolution of Alzheimer's disease-related cytoskeletal pathology in the human raphe nuclei. *Neuropathol Appl Neurobiol*. 2000; 26(6):553–567. [PubMed: 11123722]
- Smith G, de Leon M, George A, Kluger A, Volkow N, McRae T, Golomb J, Ferris S, Reisberg B, Ciaravino J, La Regina M. Topography of cross-sectional and longitudinal glucose metabolic deficits in Alzheimer's disease. Pathophysiological implications. *Arch Neurol*. 1992; 49:1142–1150. [PubMed: 1444881]
- Smith GS, Kramer E, Hermann C, Ma Y, Dhawan V, Chaly T, Eidelberg D. Serotonin modulation of cerebral glucose metabolism in depressed older adults. *Biol Psychiatry*. 2009; 66(3):259–6. [PubMed: 19368900]
- Smith GS, Ma Y, Dhawan V, Gunduz H, Carbon M, Kirshner M, Larson J, Chaly T, Belakhleff A, Kramer E, Greenwald B, Kane JM, Laghrissi-Thode F, Pollock BG, Eidelberg D. Serotonin modulation of cerebral glucose metabolism measured with positron emission tomography (PET) in human subjects. *Synapse*. 2002; 45(2):105–12. [PubMed: 12112403]
- Sossi V, De Jong M, Barker W, Bloomfield P, Burbar Z, et al. The second generation HRRT: a multi-centre scanner performance investigation. *IEEE Nucl. Sci. Symp. Conf*. 2005:2195–2199.
- Steinbusch H. Distribution of serotonin immunoreactivity in the central nervous system of the rat. *Neurosci*. 1981:557–618.
- Tabachnick, BG., Fidell, LS. *Using Multivariate Statistics*. 6. Harlow; Pearson: 2014.
- Tejani-Butt SM, Yang J, Pawlyk AC. Altered serotonin transporter sites in Alzheimer's disease raphe and hippocampus. *Neurorep*. 1995; 6(8):1207–10.
- Thomas AJ, Hendriksen M, Piggott M, Ferrier IN, Perry E, Ince P, O'Brien JT. A study of the serotonin transporter in the prefrontal cortex in late-life depression and Alzheimer's disease with and without depression. *Neuropath Appl Neurobiol*. 2006; 32(3):296–303.
- Truchot L, Costes N, Zimmer L, Laurent B, Le Bars D, Thomas-Antérion C, Mercier B, Hermier M, Vighetto A, Krolak-Salmon P. A distinct [<sup>18</sup>F]MPPF PET profile in amnesic mild cognitive impairment compared to mild Alzheimer's disease. *Neuroimage*. 2008; 40(3):1251–6. [PubMed: 18313943]
- Tsang SW, Lai MK, Francis PT, Wong PT, Spence I, Esiri MM, Keene J, Hope T, Chen CP. Serotonin transporters are preserved in the neocortex of anxious Alzheimer's disease patients. *Neurorep*. 2003; 14(10):1297–300.
- Tucker S, Ahl M, Cho HH, Bandyopadhyay S, Cuny GD, Bush AI, Goldstein LE, Westaway D, Huang X, Rogers JT. RNA therapeutics directed to the non coding regions of APP mRNA, in vivo anti-amyloid efficacy of paroxetine, erythromycin, and N-acetyl cysteine. *Current Alzheimer Research*. 2006; 3(3):221–7. [PubMed: 16842099]
- Varnäs K, Halldin C, Hall H. Autoradiographic distribution of serotonin transporters and receptor subtypes in human brain. *Hum Brain Mapp*. 2004; 22(3):246–60. (2004). [PubMed: 15195291]
- Wilson AA, Ginovart N, Hussey D, Meyer J, Houle S. In vitro and in vivo characterization of [<sup>11</sup>C]-DASB: a probe for in vivo measurements of the serotonin transporter by positron emission tomography. *Nuc Med Biol*. 2002; 29(5):509–15.
- Wolf H, Jelic V, Gertz HJ, Nordberg A, Julin P, Wahlund LO. A critical discussion of the role of neuroimaging in mild cognitive impairment. *Acta Neurol Scand Suppl*. 2003; 179:52–76. [PubMed: 12603252]
- Zhou Y, Endres CJ, Brasic James R, Sung-Cheng Huang, Wong Dean F. Linear regression with spatial constraint to generate parametric images of Ligand-receptor dynamic PET studies with a simplified reference tissue model. *Neuroimage*. 2003; 18:975–989. [PubMed: 12725772]

- Zhu CW, Livote EE, Kahle-Wroblewski K, Scarmeas N, Albert M, Brandt J, Blacker D, Sano M, Stern Y. Utilization of antihypertensives, antidepressants, antipsychotics, and hormones in Alzheimer disease. *Alzheimer Dis Assoc Disord.* 2011; 25(2):144–8. [PubMed: 20975515]
- Zweig RM, Ross CA, Hedreen JC, Steele C, Cardillo JE, Whitehouse PJ, Folstein MF, Price DL. The neuropathology of aminergic nuclei in Alzheimer's disease. *Ann Neurol.* 1988; 24:233–242. [PubMed: 3178178]

Author Manuscript

Author Manuscript

Author Manuscript

Author Manuscript

### Highlights

Individuals with mild cognitive impairment compared to controls show lower serotonin transporter binding in cortical and limbic areas, as well as in sensory and motor areas, striatum and thalamus.

Grey matter atrophy and reductions in regional cerebral blood flow in mild cognitive impairment compared to controls was more localized and less statistically robust than the reductions in serotonin transporter binding.

Lower serotonin transporter binding was associated with worse performance on tests of verbal and visual-spatial memory in individuals with mild cognitive impairment



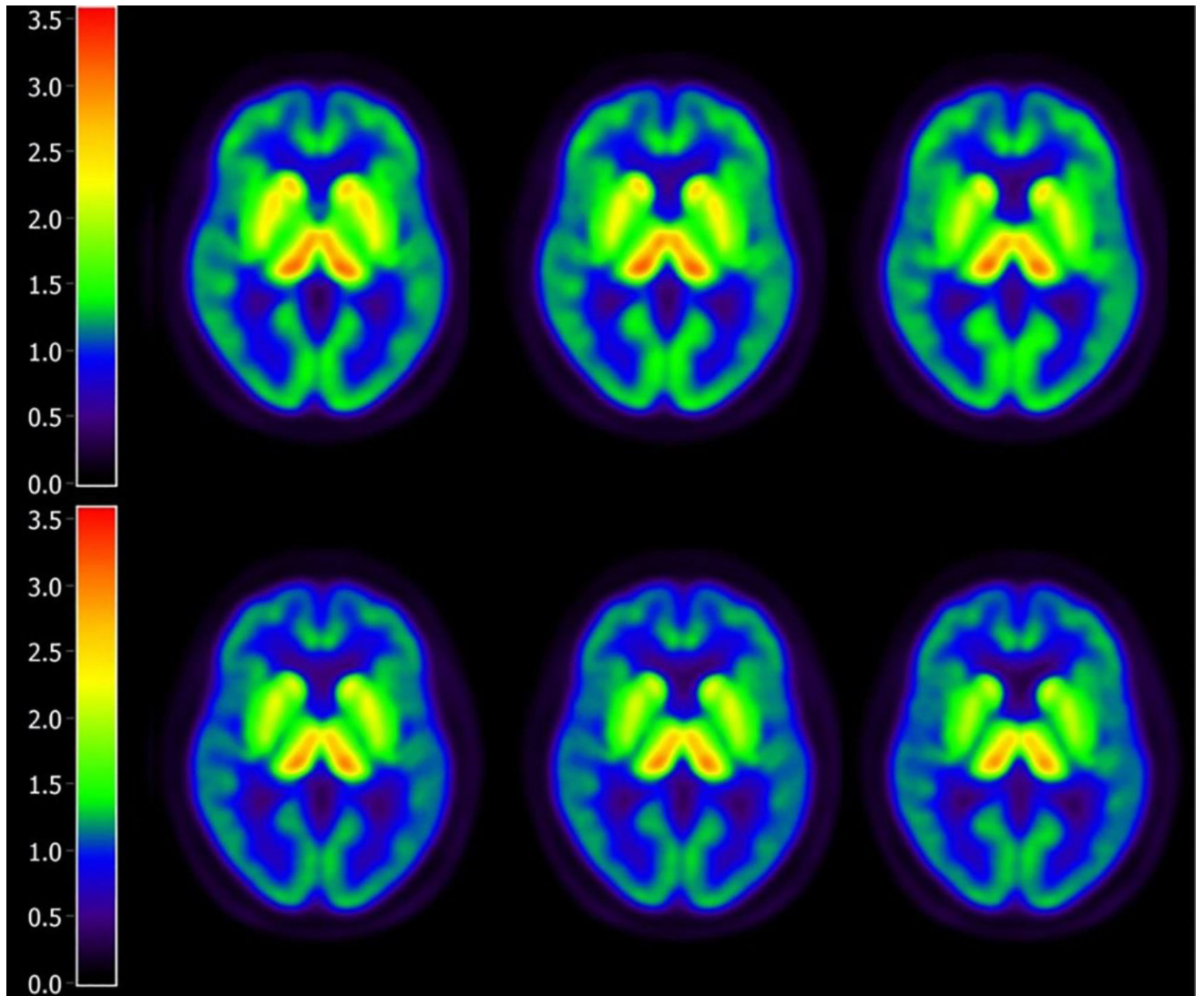
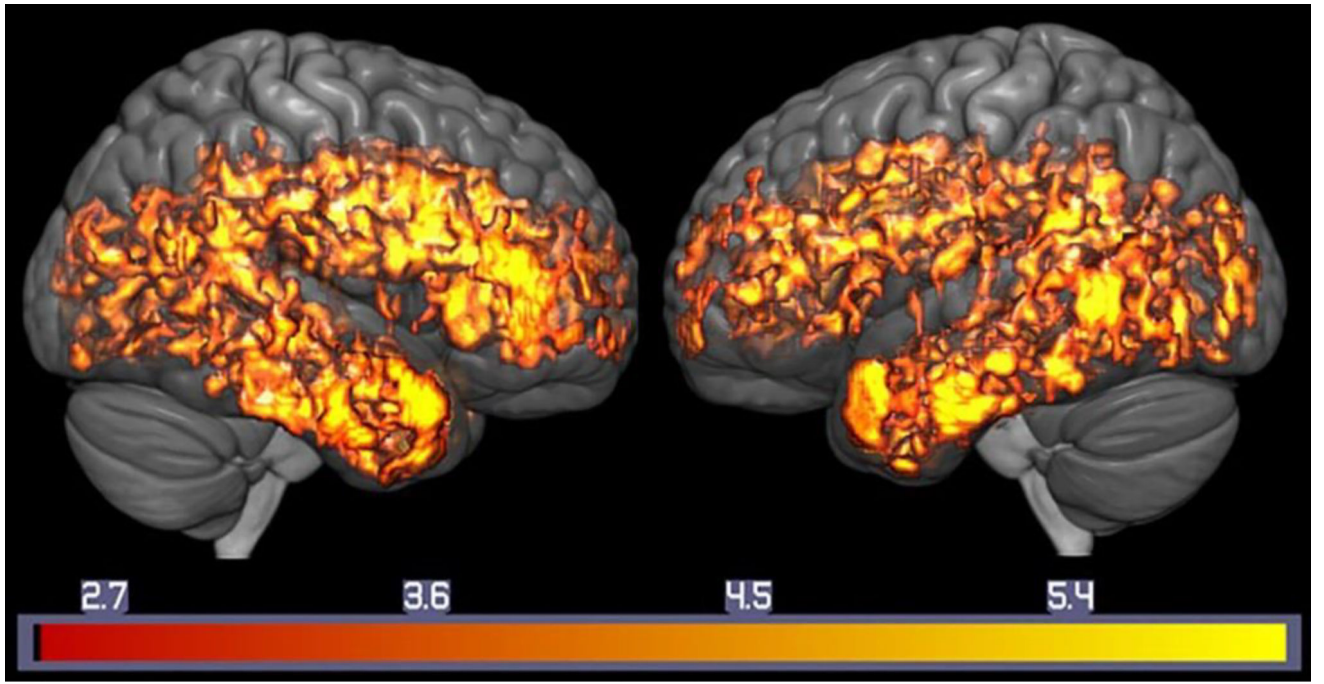
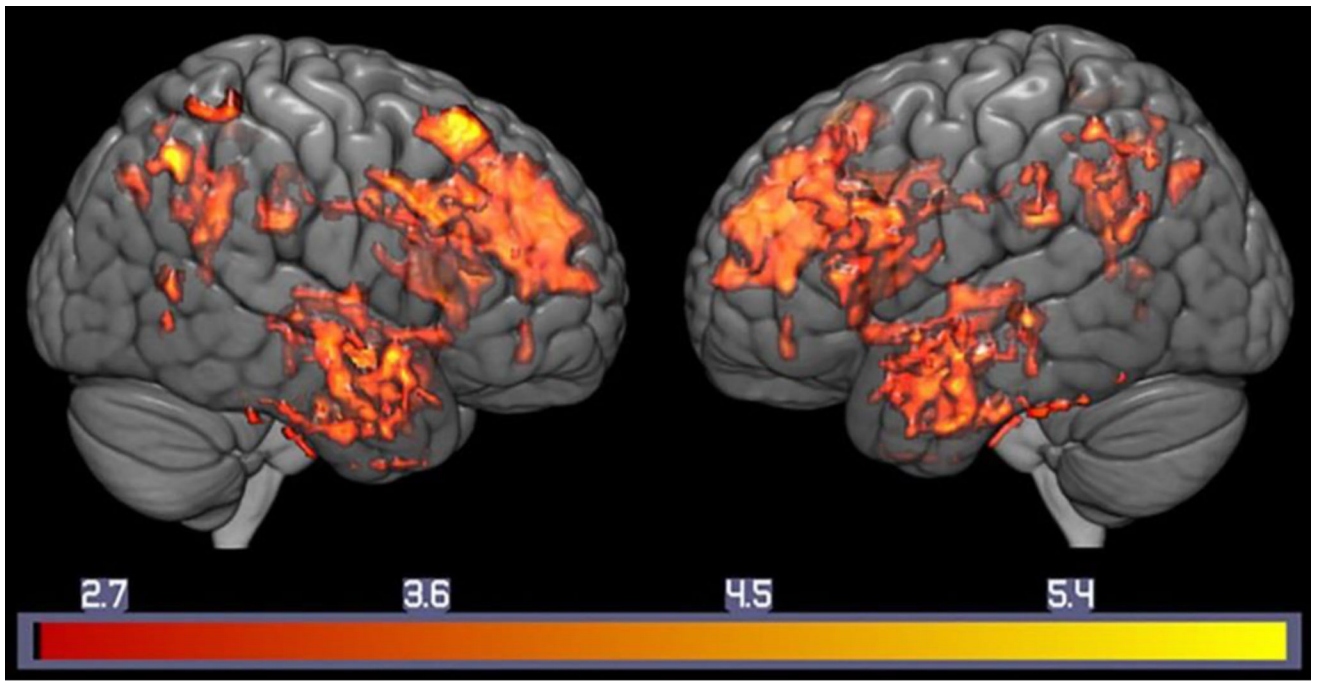


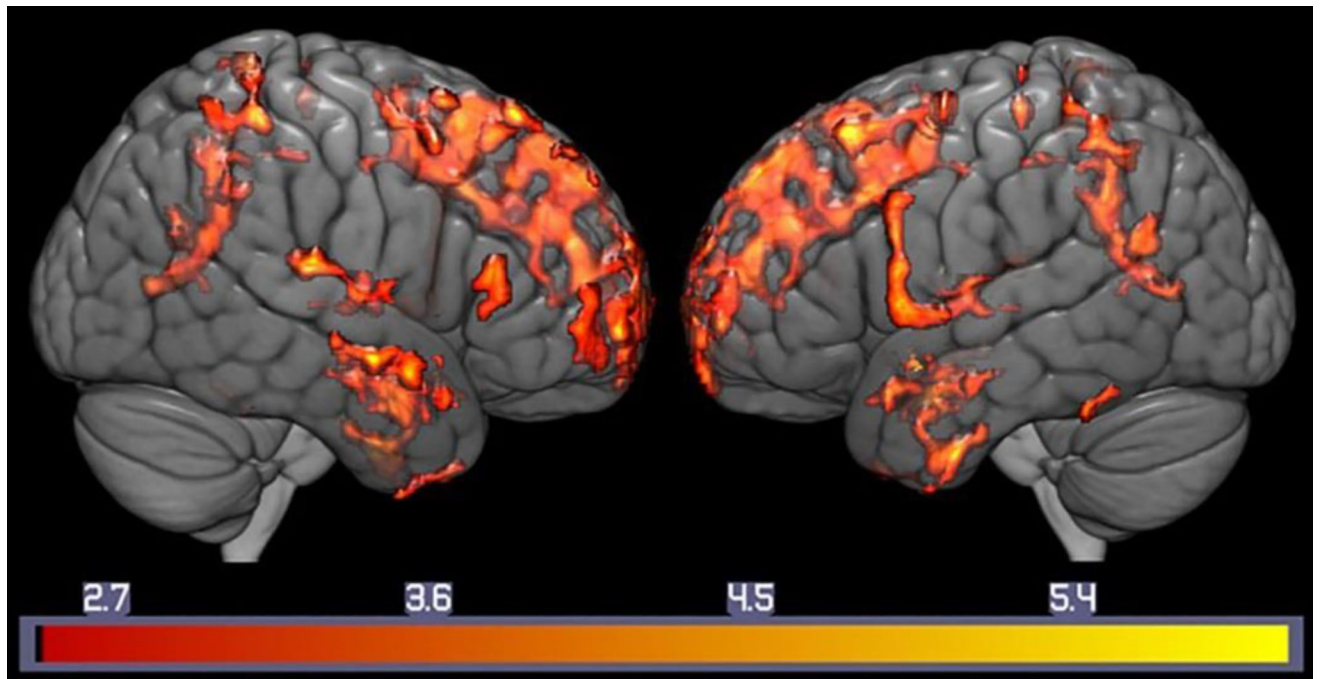
**Figure 1.** Lower Serotonin Transporters in MCI Compared to Healthy Controls. Parametric Distribution Volume Ratio Images are shown for Normal Controls (top) and MCIs (bottom). The images below represent summed images of the Normal Controls and MCIs, respectively.



a



b



**C**

**Figure 2.**

a. Lower Serotonin Transporter Binding in MCI Compared to Healthy Controls. Voxel-wise Analysis of Parametric [ $^{11}\text{C}$ ]-DASB Images. Statistically significant voxel-wise results are displayed on a three-dimensional MRI rendering.

b: Regional Correlations between Serotonin Transporter Binding and Auditory-verbal Memory in MCI. Voxel-wise Analysis of Parametric [ $^{11}\text{C}$ ]-DASB Images: Statistically significant voxel-wise results (positive correlations) are displayed on a three-dimensional MRI rendering.

c: Regional Correlations between Serotonin Transporter Binding and Visual-Spatial Memory in MCI. Voxel-wise Analysis of Parametric [ $^{11}\text{C}$ ]-DASB Images: Statistically significant voxel-wise results (positive correlations) are displayed on a three-dimensional MRI rendering.

Note: T-maps generated in SPM8 are superimposed on a MRI rendering of the ICBM 152 Nonlinear atlas (2009 version; average MPRAGE scans from 152 normal control participants). Color bars on the bottom represent the range of the T-statistic values.

**Table 1**

Demographics for Mild Cognitive Impairment (MCI) and Healthy Elderly Controls (Mean  $\pm$  Standard deviations)

|                                                                               | <b>Elderly Controls</b> | <b>MCI</b>          |
|-------------------------------------------------------------------------------|-------------------------|---------------------|
| <b>Age</b>                                                                    | 66.2 $\pm$ 7.1          | 66.6 $\pm$ 6.9      |
| <b>Sex (M/F)</b>                                                              | 15/13                   | 16/12               |
| <b>Years of Education</b>                                                     | 15.14 $\pm$ 2.6         | 15.8 $\pm$ 3.3      |
| <b>Mini Mental State Examination</b>                                          | 28.71 $\pm$ 1.3         | 27.7 $\pm$ 1.8 *    |
| <b>Neuropsychiatric Inventory (total score)</b>                               | 1.20 $\pm$ 2.2          | 4.9 $\pm$ 5.1 **    |
| <b>Hamilton Depression Rating Scale</b>                                       | 1 $\pm$ 2               | 3 $\pm$ 3           |
| <b>Total California Verbal Learning Test (CVLT) Score (Sum of Trials 1–5)</b> | 55.8 $\pm$ 10.7         | 40.5 $\pm$ 11.2 *** |
| <b>Brief Visuospatial Memory Test, Revised (Sum of Trials 1–5)</b>            | 20.0 $\pm$ 4.9          | 12.6 $\pm$ 7.1 ***  |

\* Significant between group difference ( $p < 0.05$ )

\*\* Significant between group difference ( $p < 0.005$ )

\*\*\* Significant between group difference ( $p < 0.001$ )

N=28 participants per group

**Table 2**  
Means, Standard Deviations, and Percentage Differences for Representative Regions from the SPM SERT Analysis in Mild Cognitive Impairment (MCI) and Healthy Elderly Controls

| Region: Left Hemisphere | X (mm) | Y (mm) | Z (mm) | Elderly Controls Mean (SD): | Mild Cognitive Impairment (MCI) Mean (SD): | % Difference |
|-------------------------|--------|--------|--------|-----------------------------|--------------------------------------------|--------------|
| Anterior Cingulate      | -15    | -6     | 43     | 1.11 ± 0.13                 | 0.97 ± 0.11                                | -14          |
| Medial Frontal          | -20    | 36     | 23     | 1.08 ± 0.11                 | 0.95 ± 0.09                                | -14          |
| Insula                  | -40    | -7     | 11     | 1.39 ± 0.14                 | 1.25 ± 0.14                                | -11          |
| Middle Temporal         | -44    | 2      | -34    | 1.17 ± 0.09                 | 1.07 ± 0.10                                | -10          |
| Amygdala                | -28    | -7     | -17    | 1.58 ± 0.18                 | 1.34 ± 0.25                                | -18          |
| Hippocampus             | -33    | -23    | -13    | 1.18 ± 0.12                 | 1.00 ± 0.14                                | -18          |
| Precuneus               | -14    | -65    | 19     | 1.32 ± 0.14                 | 1.17 ± 0.17                                | -13          |
| Caudate                 | -14    | 19     | 0      | 1.70 ± 0.29                 | 1.37 ± 0.24                                | -24          |
| Putamen                 | -23    | 16     | -1     | 1.79 ± 0.23                 | 1.59 ± 0.21                                | -13          |
| Thalamus                | -21    | -31    | -2     | 2.00 ± 0.26                 | 1.67 ± 0.35                                | -20          |
| Dorsal Raphe            | n/a    | n/a    | n/a    | 3.86 ± 0.73                 | 3.34 ± 0.63                                | -16          |
| Medial Raphe            | n/a    | n/a    | n/a    | 2.58 ± 0.65                 | 2.27 ± 0.47                                | -14          |

| Region: Right Hemisphere | X (mm) | Y (mm) | Z (mm) | Elderly Controls Mean (SD): | Mild Cognitive Impairment (MCI) Mean (SD): | % Difference |
|--------------------------|--------|--------|--------|-----------------------------|--------------------------------------------|--------------|
| Anterior Cingulate       | 14     | -17    | 40     | 1.12 ± 0.11                 | 0.96 ± 0.11                                | -17          |
| Medial Frontal           | 14     | 26     | 33     | 1.08 ± 0.11                 | 0.94 ± 0.11                                | -15          |
| Insula                   | 38     | -8     | 20     | 1.22 ± 0.11                 | 1.03 ± 0.10                                | -18          |
| Middle Temporal          | 53     | 5      | -21    | 0.94 ± 0.11                 | 0.84 ± 0.08                                | -12          |
| Amygdala                 | 24     | -5     | -18    | 1.67 ± 0.21                 | 1.41 ± 0.28                                | -19          |
| Hippocampus *            |        |        |        |                             |                                            |              |
| Precuneus                | 18     | -46    | 37     | 0.95 ± 0.12                 | 0.81 ± 0.10                                | -17          |
| Caudate                  | 12     | 18     | 8      | 2.14 ± 0.37                 | 1.56 ± 0.41                                | -38          |
| Putamen                  | 29     | -2     | 6      | 1.95 ± 0.21                 | 1.76 ± 0.20                                | -11          |
| Thalamus                 | 21     | -30    | 1      | 1.83 ± 0.29                 | 1.54 ± 0.25                                | -19          |

| Region: Right Hemisphere | X (mm) | Y (mm) | Z (mm) | Elderly Controls Mean (SD): | Mild Cognitive Impairment (MCI) Mean (SD): | % Difference |
|--------------------------|--------|--------|--------|-----------------------------|--------------------------------------------|--------------|
| Dorsal Raphe             | n/a    | n/a    | n/a    | 3.86 ± 0.82                 | 3.36 ± 0.68                                | -15          |
| Medial Raphe             | n/a    | n/a    | n/a    | 2.59 ± 0.62                 | 2.27 ± 0.47                                | -14          |

\* not significant

Author Manuscript

Author Manuscript

Author Manuscript

Author Manuscript



**Table 3**

Factor Analysis of SERT data in MCI and Controls

| Region of Interest     | Factor 1      |                |      | Factor 2         |                |      |
|------------------------|---------------|----------------|------|------------------|----------------|------|
|                        | Cortical DASB |                |      | Subcortical DASB |                |      |
|                        | Loading       | Bootstrap CI   | h2   | Loading          | Bootstrap CI   | h2   |
| Postcentral            | <b>0.99</b>   | (0.70 – 1.22)  | 0.90 | -0.07            | (-0.42 – 0.38) | 0.90 |
| Paracentral            | <b>0.99</b>   | (0.71 – 1.20)  | 0.83 | -0.14            | (-0.50 – 0.32) | 0.83 |
| Cuneus                 | <b>0.99</b>   | (0.67 – 1.23)  | 0.95 | -0.02            | (-0.37 – 0.48) | 0.95 |
| Precuneus              | <b>0.98</b>   | (0.67 – 1.22)  | 0.95 | -0.01            | (-0.35 – 0.46) | 0.95 |
| Superior Parietal      | <b>0.97</b>   | (0.66 – 1.21)  | 0.89 | -0.05            | (-0.39 – 0.44) | 0.89 |
| Superior Frontal       | <b>0.96</b>   | (0.65 – 1.21)  | 0.88 | -0.04            | (-0.43 – 0.46) | 0.88 |
| Pars Triangularis      | <b>0.95</b>   | (0.67 – 1.19)  | 0.84 | -0.05            | (-0.43 – 0.39) | 0.84 |
| Precentral             | <b>0.94</b>   | (0.63 – 1.21)  | 0.86 | -0.02            | (-0.42 – 0.47) | 0.86 |
| Rostral Middle Frontal | <b>0.93</b>   | (0.63 – 1.18)  | 0.88 | 0.02             | (-0.32 – 0.45) | 0.88 |
| Pars Opercularis       | <b>0.92</b>   | (0.63 – 1.18)  | 0.90 | 0.05             | (-0.30 – 0.48) | 0.90 |
| Frontal Pole           | <b>0.89</b>   | (0.58 – 1.14)  | 0.70 | -0.10            | (-0.43 – 0.34) | 0.70 |
| Caudal Middle Frontal  | <b>0.87</b>   | (0.51 – 1.20)  | 0.81 | 0.05             | (-0.39 – 0.58) | 0.81 |
| Supramarginal          | <b>0.86</b>   | (0.57 – 1.13)  | 0.87 | 0.11             | (-0.23 – 0.54) | 0.87 |
| Posterior Cingulate    | <b>0.86</b>   | (0.59 – 1.12)  | 0.85 | 0.09             | (-0.26 – 0.50) | 0.85 |
| Pars Orbitalis         | <b>0.85</b>   | (0.57 – 1.10)  | 0.76 | 0.03             | (-0.29 – 0.43) | 0.76 |
| Lingual                | <b>0.81</b>   | (0.43 – 1.18)  | 0.76 | 0.09             | (-0.52 – 0.77) | 0.76 |
| Inferior Parietal      | <b>0.74</b>   | (0.43 – 1.04)  | 0.81 | 0.23             | (-0.11 – 0.66) | 0.81 |
| Lateral Occipital      | <b>0.73</b>   | (0.35 – 1.12)  | 0.76 | 0.20             | (-0.35 – 0.81) | 0.76 |
| Superior Temporal      | <b>0.73</b>   | (0.43 – 1.04)  | 0.83 | 0.26             | (-0.09 – 0.67) | 0.83 |
| Pericalcarine          | <b>0.70</b>   | (0.32 – 1.08)  | 0.59 | 0.10             | (-0.53 – 0.79) | 0.59 |
| Ventral Diencephalon   | -0.07         | (-0.36 – 0.36) | 0.87 | <b>0.97</b>      | (0.71 – 1.18)  | 0.87 |
| Amygdala               | 0.06          | (-0.23 – 0.52) | 0.88 | <b>0.90</b>      | (0.58 – 1.11)  | 0.88 |
| Dorsal Raphe Nucleus   | -0.21         | (-0.46 – 0.19) | 0.61 | <b>0.89</b>      | (0.56 – 1.18)  | 0.61 |
| Pallidum               | 0.06          | (-0.24 – 0.52) | 0.84 | <b>0.88</b>      | (0.53 – 1.11)  | 0.84 |
| Hippocampus            | 0.22          | (-0.06 – 0.64) | 0.85 | <b>0.77</b>      | (0.38 – 1.09)  | 0.85 |

|                    | Factor 1      |                | Factor 2         |               | h2   |
|--------------------|---------------|----------------|------------------|---------------|------|
|                    | Cortical DASB |                | Subcortical DASB |               |      |
| Region of Interest | Loading       | Bootstrap CI   | Loading          | Bootstrap CI  |      |
| Putamen            | 0.19          | (-0.11 - 0.64) | <b>0.74</b>      | (0.38 - 1.01) | 0.76 |
| Caudate            | 0.24          | (-0.01 - 0.63) | <b>0.71</b>      | (0.41 - 0.96) | 0.78 |

h2 = communality. Loadings > 0.40 are presented in bold typeface. Bootstrap confidence intervals (CI) were estimated with 1000 iterations.